

Design of Thermally Induced Seizure in Journal Bearings During Start Up Using Ansys

**I.Suresh**

**M.Tech Student,
Department of Mechanical Engineering,
Visakha Technical Camps.**

**Hari Shankar Vanka**

**Assistant Professor,
Department of Mechanical Engineering,
Visakha Technical Campus.**

Abstract:

Transient thermo-elastic behavior of journal bearing during seizure is very complex and requires careful modeling of the interaction of the surface. In this project work a finite element model is used to describe the thermo-mechanical interactions of journal bearing undergoing Thermally Induced Seizure (TIS), two categories of TIS are studied. The first part deals with occurrence of seizure during start up period followed by an investigation of TIS due to the transient flow disturbance. An extensive set of parametric simulations are performed to study the effect of different parameters on TIS such as load, speed, shaft radius, operating clearance, bearing length, friction coefficient and thermal expansion coefficient. Good agreement between empirical results and the results obtained from this model attests the capability of the model and its potential for predicting thermally induced seizure phenomenon.

Introduction:

Thermally Induced Seizure in the journal bearing is a mode of failure that occurs quite suddenly and end up causing the catastrophic damage to the system. Eventhough hydrodynamic bearings are applied in practical applications over a wide range of speeds, loads etc. extensive research efforts are still going on to have better understanding of their behavior. The relative sliding motion between the two contacting

solids generally results in loss of mechanical energy due to friction. The power dissipation associated with friction is manifested in the form of heat generation at the contacting surfaces and results in an increase in temperature of sliding bodies. Many widely used mechanical components, such as bearings, seals, brakes and clutches are susceptible to frictional heating. This report investigates the effect of frictional heating on the operating clearance in a journal bearing. Operating clearance is one of the important variables in the performance of journal bearing. The variation of clearance with time is of significant practical interest particularly for situations where large frictional heat is produced as a result of dry contact. The deformation associated with expansion of the rotating shaft relative to that of the stationary bearing may be quite large, to the extent that a complete loss of clearance may take place with a catastrophic seizure.

This seizure phenomenon commonly occurs during the startup process when shaft is in direct contact with bush. Particularly susceptible to seizure are bearings that have not been used for a relatively long period of time or when the lubricant supply to the bearing is blocked thus during the startup process the shaft and the bush are in direct contact with an associated high friction coefficient. Under these circumstances one would like to be able to predict how long it takes before the seizure may set in. The objective of this work is to perform a comprehensive study of seizure in bearings during start up and when a transient flow

disturbance is occurred and alive at seizure time which is a function of various parameters. The finite element modeling is done using ANSYS .

A simplified two-dimensional analysis is performed, the analysis assumes that the contact pressure is uniform in axial direction and that no crowning or misalignment is present in the system.

The analysis of a bearing undergoing TIS during start up consist of the following steps:

1. A 2-D static contact analysis is to be performed to determine the contact forces and the contact angle.
2. A transient heat transfer analysis is to be performed to model thermal effects of dry frictional heating on the journal and the bearing.
3. A transient thermo-elastic analysis is to be performed to study the interactions of the journal-bearing pair during bearing start-up. The variation of radial clearance, contact forces and ovalization of the bearing are to be studied in this analysis.

Description of problem:

The model consists of a shaft rubbing on the inner surface of the bushing as shown in Figure 4.1. Under load frictional heat is generated at the contact between the rotating shaft and the stationary bearing. A loss of clearance occurs due to relative thermal expansion, as can be seen in the Fig.4.1 the initial cold clearance varies from zero to a maximum. During the thermal transient, the encroachment is a complex function of the various parameters, material properties and boundary conditions.

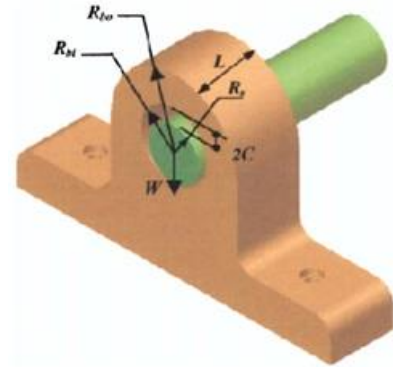


Figure 4.1 – Schematic of a journal supported on a pillow block

The total heat generated in the contact region is partitioned between the journal and bushing. When the shaft expands relative to the bushing, the increase in the frictional torque leads to an increase in the frictional heat generated at the contact. As the clearance loss progresses, a larger percentage of the total frictional heat enters the bushing due to increased area of contact and the contact conductance with the shaft.

4.1.2 Analysis Model:

The model consists of a shaft rubbing on the inner surface of the bushing as shown in Figure 4.1. The contact forces results in the generation of frictional heat on the entire surface of the shaft and in the area where it contacts the bushing inner radius. Due to the rise in temperature, the shaft expands and its encroachment to the bushing leads to a loss of clearance. At some point in time, the bearing clearance reduces to a minimum and shaft starts to encroach the bearing. Analysis show that typically during TIS, the following three phenomena occur:

- (i) The contact forces increase, increasing the heat generated.
- (ii) The contact angle increases causing a higher percentage of heat entering the bush.
- (iii) New areas of contacts are established resulting in a chain reaction of events leading to a rapid loss in the operating clearance.

The simulations presented in this work, are implemented by performing a thermal analysis and a thermo-elastic analysis in a stepwise linear fashion. The model utilized for analysis is one-half symmetry and the heat conduction in the axial direction neglected. The operating parameters used for this model are listed below:

Loading:

The loading for the static contact analysis is applied to act in the negative Y-direction on the shaft. As the model utilizes the half symmetry, a load of W/2 is applied.

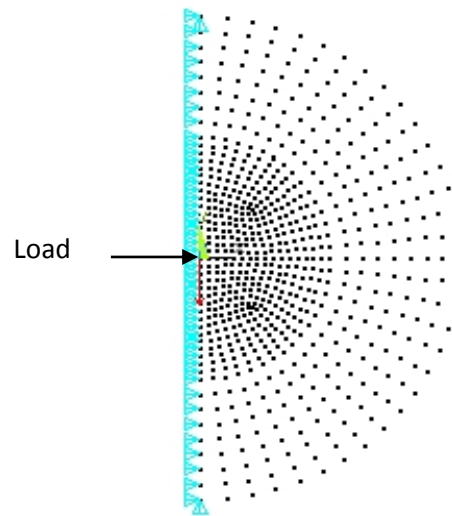
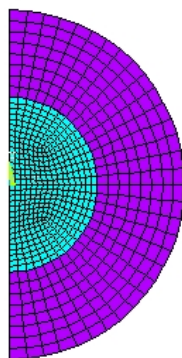


Figure4.2 Meshing of the shaft

Figure4.3 Displacement is constrained in X- an direction for all starting nodes & in Y- direction for bottom and top most nodes

Boundary Conditions:

Symmetry boundary conditions in the X direction are used to model one-half symmetry and to avoid the rigid body motion in Y direction, we are constraining two nodes on bushing in X and Y directions so that the body will not move freely in the space under the applied loads. The loading and boundary conditions are shown in Fig.4.3. The contact angle and the contact forces will be obtained from structural contact analysis. According to this model, it is calculated that the contact angle is approximately 17° for one-half symmetry. The analysis shows that for this contact angle the contact forces act only at four nodes as shown in the Figure 4.4.

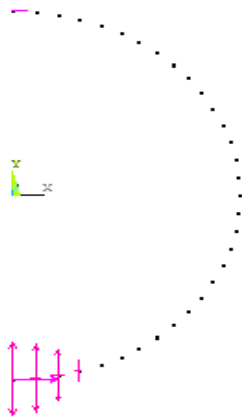


Fig.4.4 Contact force reactions due to initial static

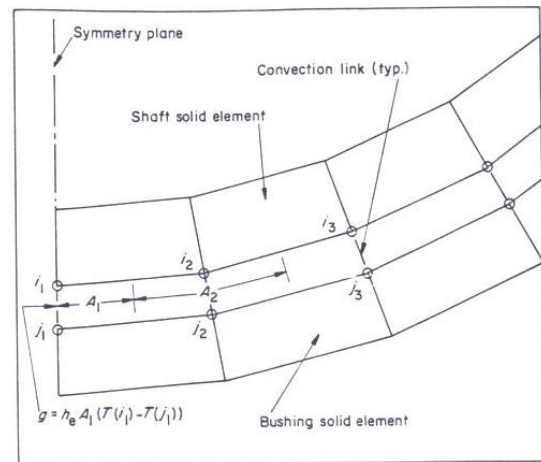


Figure 4.5. Convection link between shaft and bushing.

Step-2: Transient Thermal Finite Element Analysis

Thermal Element:

The thermal analysis is done to determine the temperature distribution in the journal-bushing pair. The journal and bushing are modeled as 4-noded solid thermal elements viz. PLANE55. The PLANE55 element has a single degree of freedom, namely temperature at each node. It is noted that the elements at the center of the shaft degenerates to triangles. This element is compatible with the 4-noded structural solid element used in the thermo-mechanical analysis. The results of the thermal analysis can be successfully exported to perform the thermo-elastic analysis. Two-node convection link element, designated as LINK34 in ANSYS used to represent the thermal contact resistance in the annular clearance. The convection link, shown in Figure 4.5, is a uniaxial element with the ability to convect heat between at its nodal points. The element has single degree of freedom, temperature, at each node point.

Material properties and loading:

The material properties required for the thermal solid elements are Thermal conductivity, k , Density, ρ and specific heat C_p . Thermal convection LINK element requires effective heat transfer coefficient (h_e) as input at the interface between the shaft and bushing. It should be noted that in the absence of contact, h_e is assumed to be equal to zero, that is no heat flow is assumed across the clearance. The area of contact is required for the convection link to calculate heat entering the bush per unit area. Since link is a line element, the method used to compute the areas can be seen in to Fig.4.5. For convection link 1, on the symmetry plane, if node i_1 on the shaft is in contact with node j_1 on the bushing the area of contact is computed based on one-half the distance to convection link 2. Likewise, for convection link 2, if node i_2 is in contact with node j_2 the area of contact is equal to one-half the distance to link 1 plus one-half the distance to convection link 3.

The loading applied to the model consists of the heat generated due to the frictional contact. The total frictional heat generated in the contact zone is:

$$Q = fu \sum P \text{-----}(1)$$

Where f is the friction coefficient of the rubbing surfaces,

P is the contact forces and

u is the velocity of rotation.

The heat generated at the interface is conducted both through the shaft and the bushing. It can be assumed that the partition of heat between the bodies is proportional to the contact area and the heat capacities of the surfaces. Therefore, the heat transferred through the shaft and bushing is:

$$Q_s = Q A_s / (A_s + A_b) \text{-----}(2)$$

And

$$Q_b = Q A_b / (A_s + A_b) \text{-----}(3)$$

The heat transferred to the stationary bush occurs over the contact arc,

$$A_b = R_b \theta_0 L \text{-----}(4)$$

While the entire surface of the rotating shaft comes into contact with the bush,

$$A_s = 2\pi R_s L \text{-----}(5)$$

Where

L is the length of the bushing in the axial direction. Since $R_s = R_b$ it can be seen from Eqs(2)-(5) that $Q_b \leq Q_s$. it is only when the bearing and shaft are in full contact, ie when $\theta_0 = 2\pi$, that $Q_b = Q_s$.

According to M.M. Khonsari and H.J.Kim it is reasonable to assume that the heat entering the shaft can be averaged over the entire circumference, therefore, the heat flux applied to the surface of the shaft is:

$$q_s = Q / (A_s + A_b) \text{-----}(6)$$

Owing to the variation of the contact with time, the heat flux applied to the bushing requires a more detailed treatment. The method used is illustrated in Fig 4. Three elements at the surface of the shaft and the corresponding surface elements of the bushing are shown. The heat flux applied to the bushing at element j would be:

$$q_b = f v ((p_i + p_{i+1}) / 2) (A_b / (A_s + A_b)) (1 / A_j) \text{----}(7)$$

Where

$q_b(j)$ = The bushing heat flux applied to surface element j .

P_i, P_{i+1} = The contact forces at gap elements i and $i+1$, respectively, as determined

from the non-linear elastic analysis.

A_j = The surface area of element j .

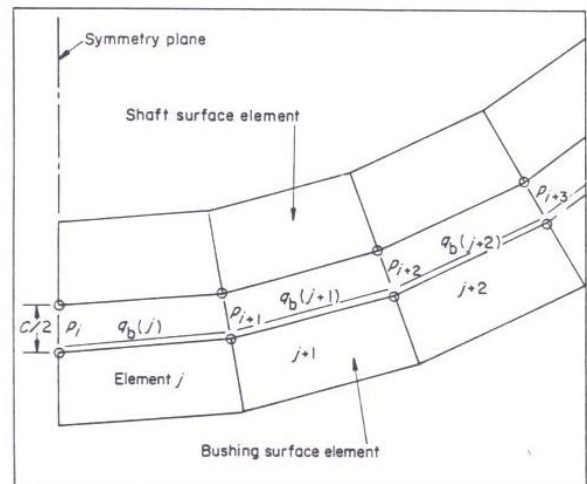
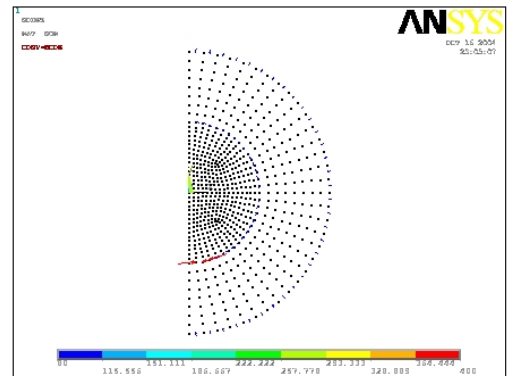


Figure 4.6 Method of applying heat flux to the bushing

Boundary conditions:

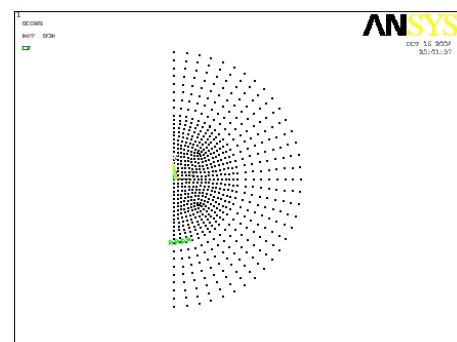
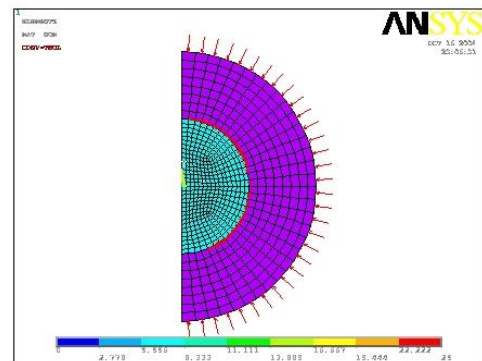
The boundary conditions used in the transient heat conduction analysis consist of the convective heat transfer coefficient at the external surfaces. The rotating shaft is heated periodically as it makes contact with the bushing. It was shown by Hazlet, that the on-off frictional heating could be applied as an average heat flux over the entire shaft surface.

Also, there is dissipation of heat by convective cooling by the air within the clearance of the journal and the bushing. In addition to the periodic heating, the shaft periodically dissipates heat as it comes into contact with the bushing. To represent the periodic heat dissipation in the finite element model, the nodes on the surface of the shaft are coupled. The temperature on the surface of the journal and the bushing at the interface is constant and is modeled by coupling the temperatures at the nodes on the interface. The outer surface of the bushing is subject to natural convection. Thermal boundary conditions and thermal loads are schematically represented in Figure 4.7.



(a) Applying heat flux

(b) Applying convection



(c) Applying bulk temperature

(d) Coupling the temperatures at the nodes on the interface

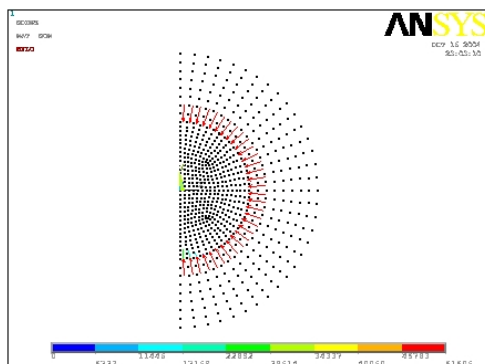


Figure 4.7 Boundary conditions and Thermal loads for transient thermal analysis

Step3: Non-linear Transient Elastic Finite Element Analysis:

Element type:

Two types of elements are used in the non-linear elastic model. The shaft and bush utilizes two dimensional isoperimetric plane stress solid element designated by PLANE42. The element is defined by four nodal points having two degrees of freedom at each node, translation in the nodal X and Y directions. The theory for the element is based on the formulation, which includes modified extra displacement shapes.

The radial clearance between the journal and the bush is modeled using two-noded contact elements, namely CONTACT12. Contact elements are used to model gap and they come into effect only when the two nodes that make the element come into contact.

Material properties and loading:

The material properties required for the solid elements are Elastic modulus, E, Poisson's ratio, ν , and Coefficient of thermal expansion, α . No material properties are required for contact elements. The loading for the non-linear thermo-elastic analysis consists of the thermal loads applied as nodal temperatures and the radial force acting on the journal. The time dependent thermal load is obtained from the results of the transient thermal analysis. The static load, W is applied to act in the negative y-direction on the shaft. As the model utilizes half-symmetry, a load of W/2 is applied.

Boundary Conditions:

Symmetry boundary conditions are used to model the one-half symmetry as shown in Fig.4.3 The constraint of the bearing on its outer surface is modeled by fixing the bearing at the node under the shaft on the outer edge of the bearing on the symmetry plane. This constraint approximates the boundary conditions of the bottom surface of the bearing support structure as shown in Figs.4.1 and 4.3.

4.1.3 Seizure Criterion:

Frictional torque is the torque resisting the driving torque exerted by the motor. When the frictional torque increases beyond the extent of the driving torque capability, it can be concluded that the journal has seized in the bearing. The present model assumes that TIS is complete when the frictional torque reaches at least 50 times the driving torque. The contact forces' acting on the gap elements at any instant of time determines the frictional torque at any time and is computed using the following equation

$$\tau(t) = 2 \cdot f \cdot R_s \sum_{i=1}^m P_i(t)$$

Where

$\tau(t)$ is the frictional torque,

f is the coefficient of friction,

R_s is the radius of the shaft,

P_i is the contact force at the i th gap element,

and

m is the number of elements in contact.

4.2 Results and Discussion:

The encroachment of the shaft on to the bushing with concomitant reduction in the clearance continues until the seizure is complete. The process is a complex, nonlinear phenomenon. Analysis shows that TIS is initiated by the ovalization of the bearing combined with the uniform outward expansion of the shaft yielding contact between the top of the shaft and the inner bushing surface. This leads to an increase in the contact forces and the formation of an extra contact area. Increase of contact forces raises the frictional heat flux and sets up a positive feedback that accelerates the loss of clearance. The increase in the frictional torque is abrupt once the ovalization of the bearing causes the shaft to encroach the bushing, as there is further loss in the operating clearance. The frictional torque increased to exceedingly large values within few seconds after the first instance of establishment of new areas of contact. The reasons for such an abrupt increase in frictional torque are:

(i) As explained previously, the increase in contact forces increases the frictional heat generated and the increase in frictional heat means that the shaft would expand more increasing the contact forces and establishing more area of contact. This process leads to a positive feedback loop and a chain reaction leading to a rapid failure due to TIS.

(ii) The operating clearance of the bearing just before seizure is reduced to a significantly

lower value compared to the steady-state operating clearance. This is due to the thermal expansion of the journal and the bearing into the operating clearance area. The available clearance just before the extra contact occurs has already reduced to an exceedingly small value.

Seizure time:

When the frictional torque increases beyond the extent of the driving torque capability, it can be concluded that the journal has seized in the bearing. The present model assumes that TIS is complete when the frictional torque reaches at least 50 times the driving torque. For the following operating parameters the frictional and driving torque values for the first 30 seconds are shown in the Table 4.1.

Operating parameters:

$W = 4400 \text{ N}$

$N = 250 \text{ rpm}$

$R_s = 25.5 \times 10^{-3} \text{ m}$

$R_b = 51.0 \times 10^{-3} \text{ m}$

$C = 0.0125 \times 10^{-3} \text{ m}$

$L = 51.0 \times 10^{-3} \text{ m}$

Table 4.1

| Time | Frictional Torque | Driving Torque |
|------|-------------------|----------------|
| 1 | 17.011 | 112.2 |
| 2 | 17.013 | 112.2 |
| 3 | 17.017 | 112.2 |
| 4 | 17.02 | 112.2 |
| 5 | 17.04 | 112.2 |
| 6 | 17.05 | 112.2 |
| 7 | 17.08 | 112.2 |
| 8 | 17.237 | 112.2 |
| 9 | 17.287 | 112.2 |
| 10 | 17.917 | 112.2 |
| 11 | 17.514 | 112.2 |
| 12 | 18.924 | 112.2 |
| 13 | 22.479 | 112.2 |
| 14 | 220.397 | 112.2 |

| | | |
|------------|-----------------|--------------|
| 15 | 613.38 | 112.2 |
| 16 | 1030.36 | 112.2 |
| 17 | 1471.072 | 112.2 |
| 18 | 1935.252 | 112.2 |
| 19 | 2422.641 | 112.2 |
| 20 | 2932.984 | 112.2 |
| 21 | 3466.028 | 112.2 |
| 22 | 4021.525 | 112.2 |
| 23 | 4599.231 | 112.2 |
| 24 | 5198.904 | 112.2 |
| 25* | 5820.309 | 112.2 |
| 26 | 6463.213 | 112.2 |
| 27 | 7127.38 | 112.2 |
| 28 | 7812.608 | 112.2 |
| 29 | 8518.654 | 112.2 |
| 30 | 9245.311 | 112.2 |

Table (4.2) Contact forces list at 12 seconds

| Node number | Contact force |
|-------------|---------------|
| 641 | 356.15 |
| 644 | 351.18 |
| 646 | 318.29 |
| 648 | 297.18 |
| 650 | 337.58 |
| 652 | 333.19 |
| 654 | 274.75 |
| 656 | 173.51 |
| 657 | 31.923 |

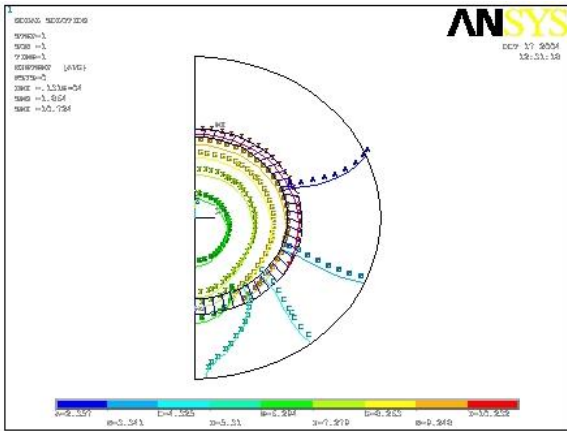
Table (4.2) Contact forces list at 25 seconds

| Node number | Contact force | Node number | Contact force | Node number | Contact force |
|-------------|---------------|-------------|---------------|-------------|---------------|
| 641 | 22734 | 652 | 23641 | 663 | 22528 |
| 642 | 23064 | 653 | 23112 | 664 | 23138 |
| 643 | 23524 | 654 | 22669 | 665 | 22990 |
| 644 | 23185 | 655 | 23968 | 666 | 22474 |
| 645 | 23541 | 656 | 23631 | 667 | 22447 |
| 646 | 23205 | 657 | 23544 | 668 | 22851 |
| 647 | 23497 | 658 | 22832 | 669 | 22448 |
| 648 | 23265 | 659 | 22710 | 670 | 22725 |
| 649 | 23391 | 660 | 23425 | 671 | 22478 |
| 650 | 23502 | 661 | 22608 | 672 | 22619 |
| 651 | 23257 | 662 | 23285 | 673 | 22537 |

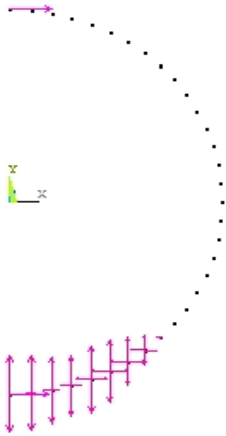
From the above table at 25 seconds of time the frictional torque reached 50 times more than the driving torque. Therefore seizure time for the above given parameters is 25 seconds.

Temperature distribution, Contact force reactions and Deformation of shaft at 12 & 25 seconds during the analysis are shown below in the Figures 4.8 & 4.9. Contact forces list at 12 & 25 seconds are shown in the Tables 4.2 & 4.3.

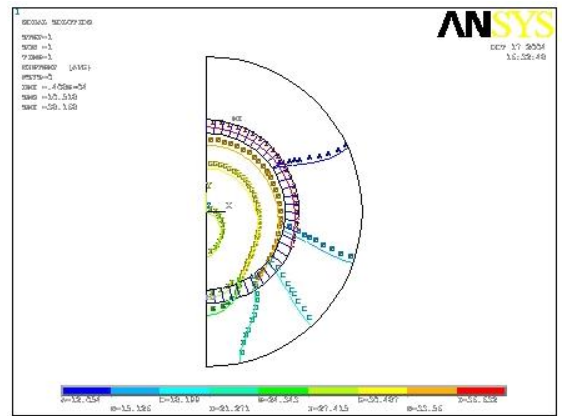
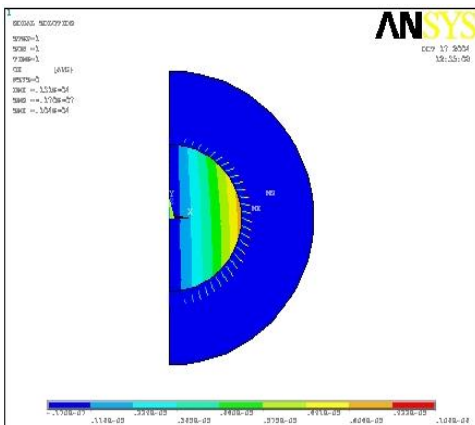
During this, it is observed that temperature rise is the function of time and those plots illustrate the onset and completion of seizure for a journal bearing during start-up.



4.8 (a) Temperature distribution

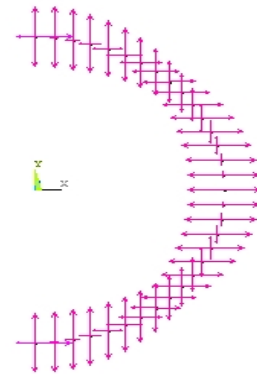


4.8 (b) Contact forces reactions



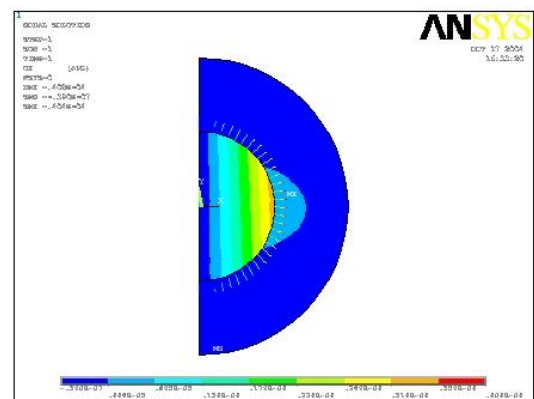
4.8 (c) Deformation of shaft

4.9 (a) Temperature distribution



4.9 (b) Contact forces reactions

4.9 (c) Deformation of shafts



Figures 4.8 & 4.9. Simulated results after 12 & 25 seconds

4.3 Verification and Analysis:

The simulated results are verified for its validity using some of the results published by Hazlett and Khonsari [8,9], Wang, Conry and Cusano [10] and Bishop and Ettles [5]. The comparisons between simulated results and some of the published results are shown in Table 4

Table (4.4) comparison of results

| Sl.No | Speed | Load | Clearance | Shaft radius | Bearing length | Thermal conductivity |
|-------|-------|--------|-----------|--------------|----------------|----------------------|
| 1 | 250 | 4400 | 1.25E-5 | 0.0255 | 0.05 | 52 |
| 2 | 1800 | 4400 | 1.25E-5 | 0.0255 | 0.05 | 52 |
| 3 | 250 | 4400 | 1.25E-5 | 0.0255 | 0.03825 | 52 |
| 4 | 250 | 4400 | 1.25E-5 | 0.0255 | 0.0255 | 52 |
| 5 | 500 | 4400 | 1.25E-5 | 0.0255 | 0.05 | 52 |
| 6 | 250 | 10000 | 1.25E-5 | 0.0255 | 0.05 | 52 |
| 7 | 560 | 160000 | 5E-5 | 0.0781 | 0.1562 | 30 |
| 8 | 560 | 160000 | 50E-5 | 0.0781 | 0.1562 | 30 |
| 9 | 1000 | 1E6 | 0.5E-5 | 0.5 | 1 | 52 |
| 10 | 1000 | 1E6 | 2.5E-5 | 0.5 | 1 | 52 |

To gain further insight into the TIS behavior, we plot the change in the operating clearance as a function of time based in Dufrane and Kannel's equation (4.1) and the simulated results in the present study are shown in Figure 4.10 for two heat partitioning factors ($n = 0.5$ and 1). ANSYS 7.1 calculates the heat-partitioning factor based on the thermal mass and material properties at the contact area such that there is continuity of temperature and flux at the contact interface.

A heat partitioning of 1 is not reasonable as it means that all the frictional heat generated would be transmitted into the shaft. The analysis done by

Dufrane and Kannel [6] did not consider the expansion of the bushing, the thermal expansion of the shaft was only considered. Also, the bushing was rigidly constrained. As

the present study has considered the bushing constraint the outward expansion of the bushing, the seizure times were larger than the values obtained using Equation (4.1) used by Dufrane and Kannel. From Figure 4.10, it can be seen that the present model compares close to Dufrane and Kannel's model when a heat-partitioning factor of 0.5 is used in Equation (1). The seizure time formula developed in this study predicts the loss of clearance with time is not a linear process. Whereas Equation (4.1) implies that TIS occurs regardless of the size of the clearance, the predicted results here reveal that this is not true for large clearances. This physically realistic prediction was first discussed by Khonsari and Kim [18].

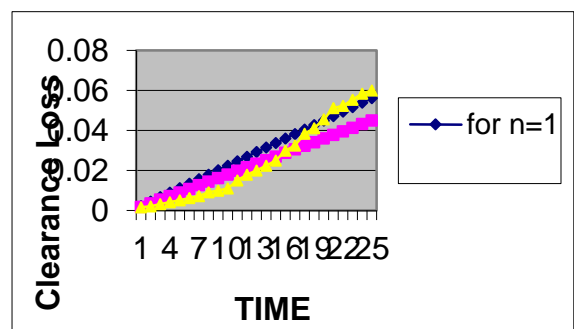


Figure 4.10 Comparison of seizure time with Dufrane and Kannel's model and the Present model. Note: n = heat partition factor

4.4 Thermoelastic behavior of journal bearings undergoing seizure:

Extensive numerical results are presented for the behavior of journal bearing under going seizure. Included in the results is a sensitivity study performed to investigate the influence of various bearing parameters and operating conditions on the on set of seizure. It is demonstrated that high shaft speeds could lead to a very rapid seizure when the bearing is subjected to dry sliding. The transient thermoelastic behavior of journal bearing seizure is very complex and requires careful modeling of the interaction of the surfaces.

In the above sections the details of a finite element model and numerical procedure for the analysis of journal bearings undergoing seizure are presented. In this section extensive numerical simulations for a number of test cases are presented. The analysis involves numerous iterations. Therefore, output from such an analysis can be voluminous.

In this section concentration was focused on the following analysis: frictional torque versus time, a sensitivity study of the seizure time depends upon the bearing parameters and operating conditions.

(a) Frictional torque versus time:

A plot of the frictional torque versus time is shown in Figure 4.12. Each point on the plot is determined by first summing the contact forces at the gap elements. Prior to encroachment the sum of the contact forces is equal to half the static shaft load, P. Clearance loss begins to occur at about 25 s. This is denoted by a rise in the frictional torque. Dufranel developed an expression for the clearance change using a simplified one-dimensional analysis of the problem. Rewriting

this expression and solving for the seizure time yields the following equation

$$t_{ss} = \frac{C\rho C_p}{2(1+\nu)\alpha q_s} \cdot \frac{1}{\left[(n-1)\left(\frac{R_{bo}}{R_s} - \frac{R_s}{R_{bo}}\right)^{-1} + n \right]}$$

For the above given parameters t_s is equal to 15 seconds. However, from Figure 4.11, seizure may not occur until 28seconds into the transient. Therefore, it can be confirmed that the simplified one-dimensional analysis provides a conservative estimate of the seizure time.

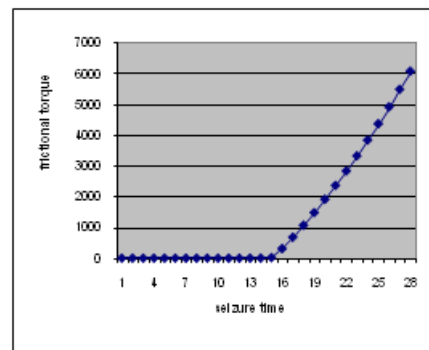


Figure 4.11 Variation of frictional torque w.r.t. time.

(b) Lubricated contact:

The journal bearing seizure analysis has been performed assuming that dry sliding occurs between the shaft and bushing. In a typical fluid film bearing the surface of the shaft and bushing are completely separated by Film of oil. The major effect of the lubricant is to provide a low friction coefficient and increased internal cooling. The friction coefficient for a lubricated contact is around 0.005 as compared to the value of 0.15 used for the dry sliding case. The heat generated at the rubbing surfaces is directly proportional to the frictional coefficient. Therefore, when the contact is lubricated, the magnitude of the

clearance loss would be much less than the dry friction case. In addition, lubricant normally provides some internal cooling. A plot of the frictional torque versus time is shown in Fig 4.12 for the different frictional coefficient values.

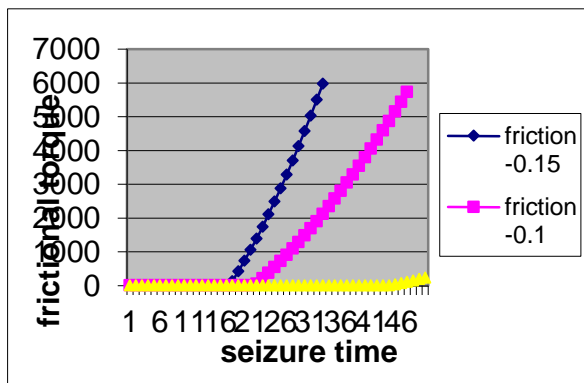


Figure 4.12 Effect of Friction coefficient on Frictional torque

(c) Sensitivity study:

The analysis using the given parameters has shown that in the absence of lubrication, seizure of the journal could occur in less than 30 s of operation. The length of time, for which dry sliding can be tolerated, may vary significantly from one design to another. To understand the influence on seizure of the various parameters, a sensitivity study is performed.

Bushing length:

One of the design parameters of hydrodynamic journal bearings is the ratio of the bushing length, L, and the shaft radius, Rs. The value of L/Rs used in the analysis is 2.0. This parameter appears in a dimensionless form of the so-called Reynolds. Equations, which describe the pressure distribution in the fluid film around the circumferential and axial directions. Normally bearings with $L/2R_s = 1$ are called finite bearings in

that both the axial and circumferential pressures are important. Accordingly, bearings with $L/2R_s < 1$ and $L/2R_s > 1$ are classified as short and long bearings, respectively. Reducing the bushing length results in greater frictional heat generation and therefore shorter seizure times. A decrease in L/Rs is shown to result in a nearly proportional decrease in the seizure times. A plot for frictional torque versus time is shown in Fig 4.13 for the different lengths of bearing.

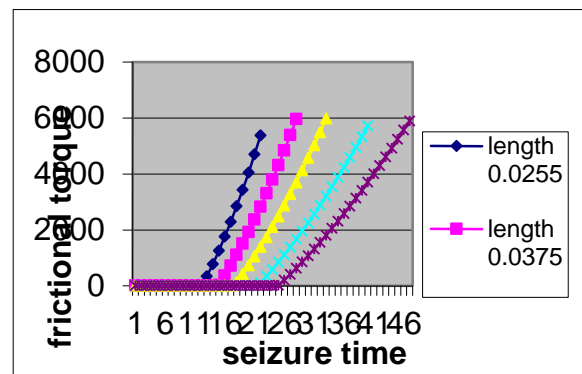


Figure 4.13 Effect of bearing Length on Frictional torque

(ii) Clearance:

Operating clearance is one of the important variables in the performance of journal bearing. The variation of clearance with time is of significant practical interest particularly for situations where large frictional heat is produced as result of dry contact. The deformation associated with expansion of the rotating shaft relative to that of the stationary bearing may be quite large, to the extent that a complete loss of clearance may takes place with a catastrophic seizure. Variation of the frictional torque with respect to time for different clearance values is shown in Figure 4.14

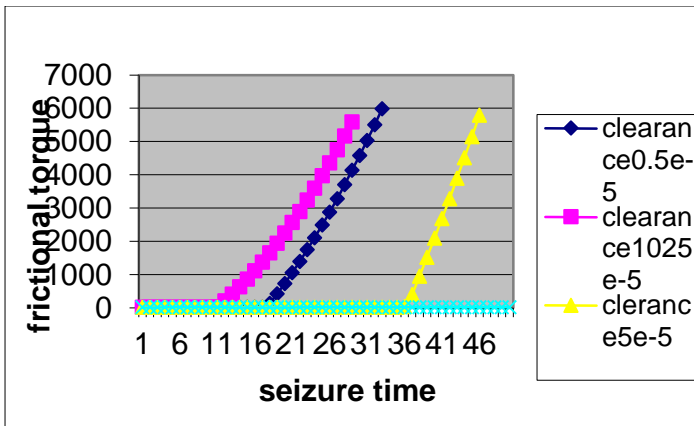


Figure 4.14 Effect of Clearance on Frictional torque

(iv) Speed: All the simulation studies are for a shaft speed, N of 200 rev/min. For many practical applications much higher speeds can be expected. The frictional heat is proportional to N, high operating speeds will have a significant impact on the time to seizure.

The FEA is run for N = 1800 rev/min. The analysis shows that increasing the shaft speed by factor of 7.2 can result in over a ten-fold decrease the time it takes for the shaft to seize. Equation 4.1 derived from the I-D analysis, indicates that the relationship between seizure time and shaft speed is linear.

The 2-D analysis points out the importance of operating the shaft at low speeds during times when the bearing is most susceptible to dry sliding. The variation of frictional torque for different speeds are shown in Figure 4.15

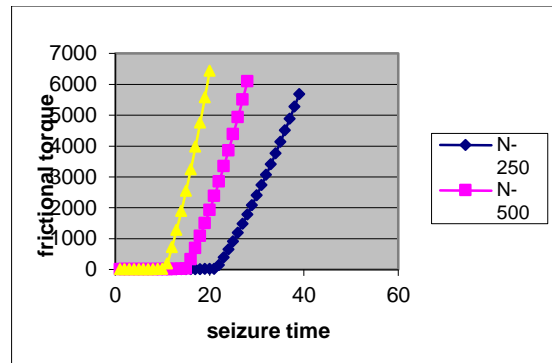


Figure 4.15 Effect of Speed on Frictional torque

(iv) Load:

Frictional torque is greatly influenced by the load. Load must be depends on the operating parameters. We must have some limitation to the load for different operating parameters. For the above given parameters the variation of frictional torque for the different load values are shown in the Figure 4.16

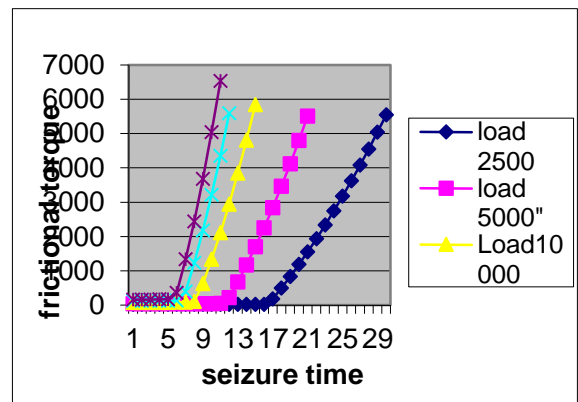


Figure 4.16 Effect of Load on frictional torque

Conclusions:

TIS in Journal Bearings During Start Up:

When rotating machinery that is supported on fully lubricated bearings are started up from rest, the lubrication flow may not have been established and there would be metal-to-metal contact. The effect of the dry sliding during start-up was analyzed by studying the effect of start-up friction on the bearing

operating parameters such as clearance loss and frictional torque by a thermoelastic finite element model. A series of simulations were performed by varying the operating parameters to give insight in to the system. The 1D Equation predicts a linear relation between the seizure time and the operating clearance. This means that the bearing will seize even if the clearance is very large and it gives the conservative results. This 2D analysis gives detailed finite element analysis to gain insight into the nature of the contact forces and encroachment of the mating pair leading to TIS of a dry bearing during start up. Thermo elastic behavior of journal bearing undergoing TIS were studied for the different operating parameters to gain insight in to the system.

References:

1. **Ling F. F. and Saibel E.** Thermal aspects of galling of dry metallic surfaces in sliding contact. *Wear*, 1958, **1**, 80-91.
2. **Gecim B. and Winer W. O.** Steady State Temperature in a Rolling Cylinder Subject to Surface Heating and Convective Cooling. *ASME Journal of Tribology*, 1984, **106**, 120-127
3. **Patula E. H.** Steady State temperature Distribution in a Rotating Roll Subject to Surface Heat Fluxes and Convective Cooling. *ASME Journal of Tribology*, 1981, **103**, 36-41
4. **Ulysee P. and Khonsari M. M.** Thermal Response of Rolling Components Under Mixed Boundary Conditions: An Analytical Approach, *ASME Journal of Heat Transfer*, 1993, **115**, 857-865
5. **Bishop J.L. and McC. Ettles C.M.** The seizure of journal bearings by thermoelastic mechanisms. *Wear*, 1982, **79**, 37-52
6. **Dufrane K. and Kannel J.** Thermally induced seizures of journal bearings. *ASME Journal of Tribology*, 1989, **111**, 288-92
7. **Khonsari M.M. and Kim H.J.** On thermally induced seizure in journal bearings. *ASME Journal of Tribology*, 1989, **111**, 661-7
8. **Hazlett T.L. and Khonsari M.M.** Finite element model of journal bearing undergoing rapid thermally induced seizure. *Tribology International*, 1992a, **25**, 177-82
9. **Hazlett T.L.** Thermoelastic behavior of journal bearing undergoing seizure *Tribology International*, 1992a, **25**, 182-87
10. **Wang H., Conry T.F. and Cusano C.** Effects of Cone/Axle Rubbing Due to Roller Bearing Seizure on the Thermomechanical Behavior of a Railroad Axle. *ASME Journal of Tribology*, 1996, Vol.118, pp.311-319
11. **Wang Q.,** Seizure Failure of journal-bearing conformal contacts. *Wear*, 1997, **210**, pp.8-16.
12. **Lacey S. and H. Kawamura H.,** Bearings for Aircraft Gas Turbine Engines (Part 1), *NSK Technical Journal – Motion and Control*, 1998, **5**, pp. 1-8
13. **Pascovici M.D., Khonsari M.M. and Jang J.Y.,** On the Modeling of Thermomechanical Seizure. *ASME Journal of Tribology*, 1995, **117**, 744-7
14. **Jang J.Y., Khonsari M.M. and Pascovici M.D.,** Thermohydrodynamic Seizure: Experimental and Theoretical Analysis. *ASME Journal of Tribology*, 1998, **120**, 8-15



15. **Cook R.D., Malkus D.S. and Plesha M. E.**, Concepts and Applications of Finite Element Analysis, *John Wiley and Sons, 1989, Third Edition*

16. **Incropera F.P. and Dewitt D. P.** Fundamentals of Heat and Mass Transfer, *John Wiley and Sons, 1996, Fourth Edition*

17. ANSYS 5.7 Online Users Manual, 2001, *ANSYS Inc*

18. **Khonsari M.M. and Kim H.J.**, Discussion on paper titled "Thermally induced seizures of journal bearings" by Dufrane K. and Kannel J., *ASME Journal of Tribology*, 1989, **111**, 292

19. **Mills A.F.**, Heat and Mass Transfer, *Richard D Irwin Inc.*, 1995

Author's Details:

Mr.I Suresh is a P.G Student of Mechanical Department of Visakha Technical Campus. He Has Done His B.Tech from Gonna Institute of Information Technology And Sciences (GIITS) Visakhapatnam .India.

Mr. Hari Sankar Vanka Is Born in Andhra Pradesh, India. He Has Received M.Tech. [CAD /CAM] From JNTU, KAKINADA. Ap, India. He Is Working As Assistant Professor In Mechanical Engineering Dept, Visakha Technical Campus, Narava, and Visakhapatnam. India.